

PREDICTING GALLOPING AMPLITUDES: II

By A. S. Richardson, Jr.¹

ABSTRACT: The application of wind tunnel data to the calculation of vibration amplitudes includes the effect of structural damping. The linear theory is also reviewed and compared to the nonlinear theory. The asymptote for a vibration limited only by aerodynamic drag is approached when the system damping is near zero. The limit cycle predicted by theory is compared with the limit cycle found in wind tunnel tests. The agreement is good. Additional effects of span distribution are identified for further study. The role of mechanical system damping is shown to diminish as the wind speed increases above the critical wind speed. The critical wind speed is the same no matter which theory, linear or nonlinear, is used. An approximate describing function is introduced in closed form, which is based on maximum lift and lift reversal angle.

INTRODUCTION

The first part of the paper (Richardson 1988) is a description of the generalized methodology and some practical illustrations of its use. For simplicity, that part did not consider the effect of structural damping. The amplitude limit cycle is the result of energy balance by aerodynamic means. It is a nonlinear version of the more familiar (linear) den Hartog criterion.

All structures have some finite structural damping. The quantitative measure of it is: (1) Log-decrement; (2) loss factor; or (3) damping ratio. All are linearly related in the ratio 2π to 2 to unity. In the galloping of a single-degree-of-freedom system, linear theory has shown that the damping and the critical wind speed are proportional. The so-called Scruton number has also been identified as *mu-g* by Richardson (1963) and reduced damping by Parkinson (1963). The parameter is nondimensional. It is the product of "relative density" by damping. The relative density is the ratio of a unit mass of the vibrating member to the mass of displaced air (or water) having the same volume as the unit mass of the vibrating member.

In most cases, the *mu-g* parameter may be interpreted as "the minimum damping required for stability" (Richardson 1963). It is a function of aerodynamics; initial angle of attack; and in the case of multi-degree-of-freedom, a function of frequency ratio, radius of gyration, and center of gravity offset. None of the multi-degree-of-freedom effects are considered here. The only additional effect considered is the effect of structural damping, *mu-g*.

ANALYSIS

An illustration of the effect that damping has on the stability of the D-section shape may be seen in Fig. 1. This is based on the linear analysis. It is clear that two regions of instability exist, one near the initial angle of attack $\alpha_0 = 27^\circ$, and the other near $\alpha_0 = 90^\circ$. An instability at $\alpha_0 = \text{zero}$

¹Pres. Research Consulting Associates, 3 Wingate Rd., Lexington, MA 01273.

Note. Discussion open until April 1, 1989. Separate discussions should be submitted for the individual papers in this symposium. To extend the closing date one month, a written request must be filed with the ASCE Manager of Journals. The manuscript for this paper was submitted for review and possible publication on April 22, 1987. This paper is part of the *Journal of Engineering Mechanics*, Vol. 114, No. 11, November, 1988. ©ASCE, ISSN 0733-9399/88/0011-1945/\$1.00 + \$.15 per page. Paper No. 22956.

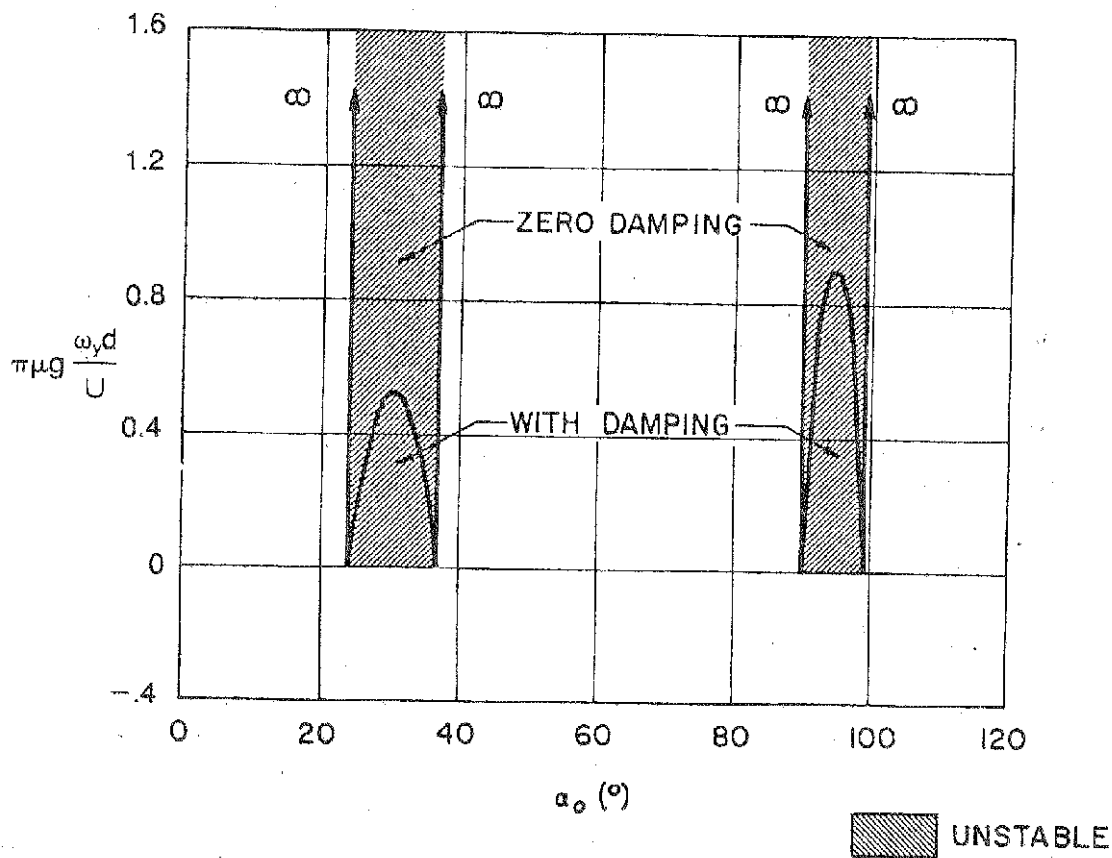


FIG. 1. Stability Boundary for D-Section Based on Single-Degree-of-Freedom (Vertical) Analysis

degrees exists only if an initial displacement is given to the vibrating member, while the two shown in Fig. 1 actually did start from rest. The bands of instability are limited by finite damping. If the $\mu u-g$ reduced frequency product exceeds 0.5 at the low angle of attack, or 0.9 at the high angle of attack, no instability (galloping) is predicted. Thus, while the den Hartog criterion correctly predicts the range of instability in terms of the angle of attack, it remains for the $\mu u-g$ reduced frequency product to identify the wind speed. The wind speed thus identified is called the "critical wind speed," because it is the lowest wind speed at which galloping can occur.

Once the critical wind speed is exceeded, it becomes necessary to consider non-linear effects—otherwise, linear theory predicts infinite amplitudes, even with finite damping. The nonlinear effects considered here are only within the range of the (nonlinear) lift curve versus angle of attack. Further, for simplicity, initial angle of attack is considered zero, and the bluff shape is symmetrical about $\alpha_0 = 0$. Shapes that qualify are: (1) The square; (2) the iced conductor; (3) the figure eight. The first two were studied in Part I (Richardson 1988).

The generalized methodology is not limited to these shapes, of course, nor is it limited to the initial angle of attack $\alpha_0 = \text{zero}$. Many other bluff shapes may be of interest (see Richardson 1986). Other initial angle of attack cases can be treated as well, though the mathematics gets somewhat involved.

The energy input from the wind to any system undergoing cross-wind oscillation in a single degree of freedom is found by integrating the com-

ponents of lift and drag over a complete cycle (Richardson 1988)

$$E = \frac{qA}{\Omega} \int_0^{2\pi} (C_L \cos \alpha + C_D \sin \alpha) \frac{dy}{dt} d(\Omega t) \dots \dots \dots (1)$$

The symbols are identified in Appendix II.

The instantaneous angle of attack and the displacement are related

$$\frac{dy}{dt} = -\Omega Y \sin(\Omega t) \dots \dots \dots (2)$$

$$\alpha = a \sin(\Omega t) \dots \dots \dots (3)$$

It is seen that the angle of attack and transverse velocity are out of phase by 180°. It is precisely this connection that leads to the den Hartog criterion (Richardson 1963).

According to Part I, the drag coefficient is constant during a complete cycle, but the lift coefficient is represented by

$$C_L = S_1 \sin(\Omega t) \dots \dots \dots (4)$$

Eq. 4 has employed the condition of bluff body symmetry about the initial (zero) angle of attack.

If it is assumed that the lift curve is itself a sine curve centered on the initial (zero) angle of attack

$$C_L = -A_m \sin\left(\frac{\pi\alpha}{a_0}\right) \dots \dots \dots (5)$$

$$C_L = -A_m \sin\left[\left(\frac{\pi}{a_0}\right)(a \sin \Omega t)\right] \dots \dots \dots (6)$$

And, by definition of S_1 (the "describing function")

$$S_1 = \frac{-1}{\pi} \int_0^{2\pi} A_m \sin\left[\left(\frac{\pi}{a_0}\right)(a \sin X)\right] \sin X dX \dots \dots \dots (7)$$

But the integral (on X) is identified in closed form as the Bessel function of the first kind, J_1 (Jahnke 1945), and "the describing function," S_1 , becomes, simply

$$S_1 = -2A_m J_1\left(\frac{\pi a}{a_0}\right) \dots \dots \dots (8)$$

This can be applied to any symmetrical bluff shape, provided the lift curve can be characterized by the two parameters A_m and a_0 , which are, respectively, the C_L max and the lift reversal angle of attack. The C_L max is sensitive to Reynolds number, as noted in Part I (Richardson 1988). The C_D is not so sensitive, nor is the lift reversal angle, a_0 . It is noted that the initial slope of the lift coefficient, given by $-A_m\pi/(a_0)$, must be numerically larger than the drag coefficient, C_D . Otherwise, no gallop is possible.

Having simplified the right hand side of Eq. 1, the left hand side—from Part I (Richardson 1988)—is seen as follows:

$$\frac{E}{qAY} = -S_1(J_0 - J_2) - 2 C_D J_1 \dots \dots \dots (9)$$

where the S_1 is to be interpreted as previously derived, in Eq. 8.

When $E > 0$, energy flows into the system from the wind. Only the internal structural damping can absorb it (in the absence of any vibration "dampers"). The absorbed energy in a vibrating single-degree-of-freedom system is just equal to two times the log-decrement times the maximum system kinetic energy. Many classic textbooks may be consulted to verify that truth (Simiu 1986). The system kinetic energy is one-half times the generalized mass times the square of transverse velocity, dy/dt . By making use of the relations between transverse velocity and angle of attack, the expression (Eq. 9) becomes

$$(2\pi\mu\delta)\left(\frac{fd}{U}\right) = -\left(\frac{1}{a}\right)[S_1(J_0 - J_2) + 2C_D J_1] \dots \dots \dots (10)$$

This equation provides the basic relationship between damping (log-decrement), δ (relative density) μ , reduced frequency (fd/U), and aerodynamic parameters characterized as $C_L \max = A_m$, lift reversal angle (a_0), and the limit cycle, a . The limit cycle is the maximum steady-state dynamic angle of attack, a .

In most cases of practical interest, the limit cycle angle of attack is less than 30° , so that the gallop amplitude may be found from

$$\left(\frac{\Omega Y}{U}\right) \cong a \dots \dots \dots (11)$$

ILLUSTRATIVE EXAMPLE

The application of Eq. 10 is best illustrated by a typical example. The square cross section is chosen for that purpose. It was already noted in Part I (Richardson 1988) that the present method can easily account for effects of Reynolds number. The illustrative example will bring out that point again.

The damping required function is Eq. 10. The right hand side is a function of aerodynamic parameters, S_1 and C_D , and by Eqs. 5 and 7, the S_1 is a function of maximum lift coefficient, A_m , and lift reversal angle, a_0 . The Bessel functions can be found from tables (Jahnke 1945) or calculated from their series representation. If a personal computer is available, the latter course will be the most efficient.

Here, the square section is considered at two Reynolds numbers, high and low. The high Reynolds number is considered to be near 100,000 and the $C_L \max$ is put equal to unity. The lift reversal angle of attack is 38° . These two parameters are sufficient to specify the describing function, $S_1(a)$ (see Eq. 8). The low Reynolds number is considered to affect only the $C_L \max$, and it is assumed to be $A_m = 2/3$. The two cases are seen in Fig. 2. (High $R = A$, Low $R = B$)

The damping required to prevent galloping is given by the intercept on the ordinate. Its numerical value is 3.05 (high Reynolds number) and 1.45 (low Reynolds number). The former may be compared with numerical values of 2.8 found by Parkinson (1963). The first figure also agrees with the den Hartog number found from Eq. 5, together with a drag coefficient of $C_D = 1.7$.

The second figure at low Reynolds number is close to the numerical value found by Dugundji (1976). Thus, more than twice as much damping is re-

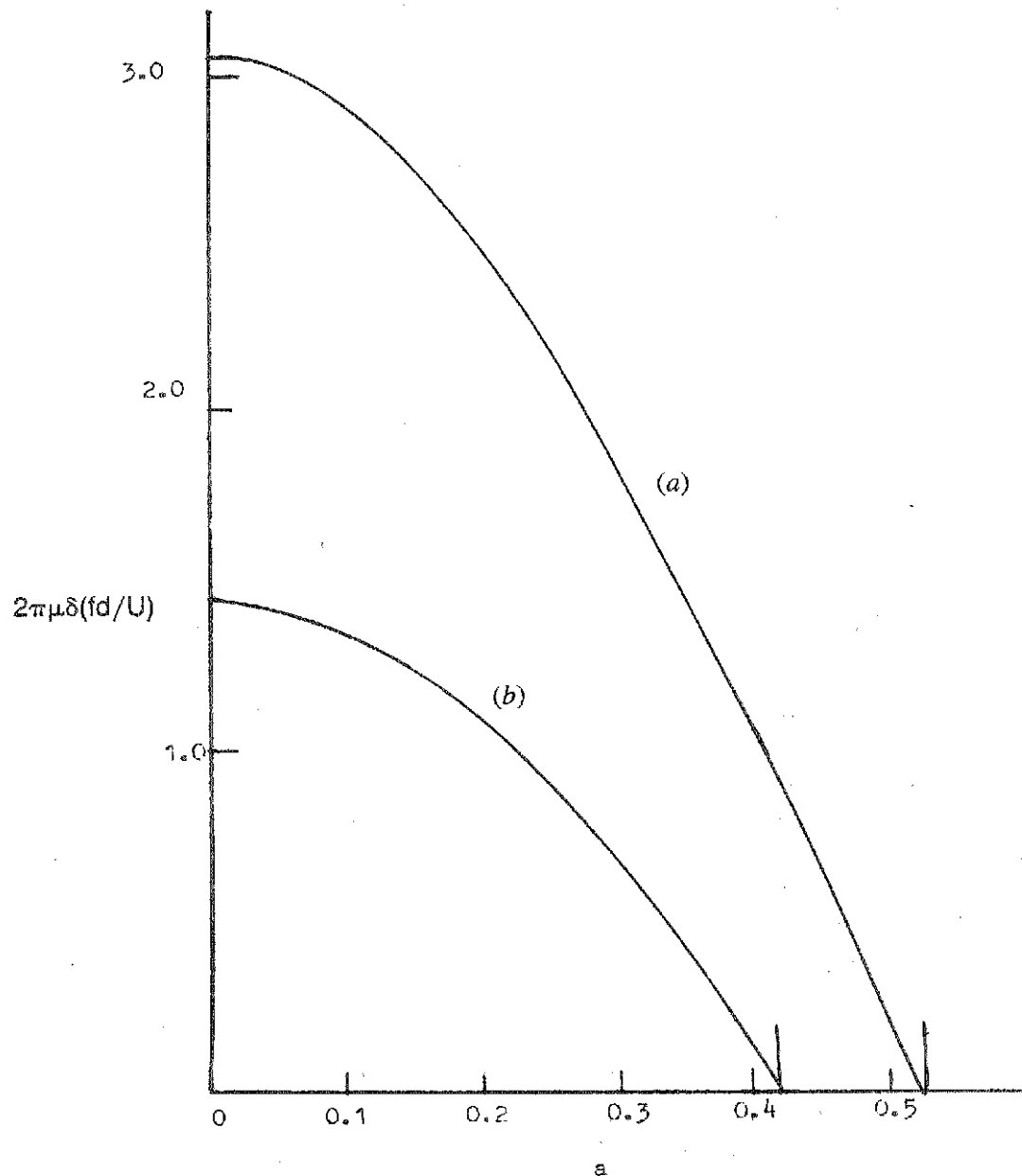


FIG. 2. Damping Required for Square Section—Initial Angle of Attack = 0

quired to prevent galloping at high Reynolds number. Further, the damping required at small amplitude ($a = 0$) agrees with the linear theory.

As the system damping decreases from its value (at $a = 0$) while wind speed is constant, there is an increase of the galloping amplitude, until at zero damping, the abscissa axis intercept is found. For high Reynolds number the intercept is 0.52, while for low Reynolds number the intercept is 0.41. These are the "free-running gallop" amplitudes, so named because they are limited only by the aerodynamic damping due to drag. In Part I (Richardson 1988), a numerical value of $a = 0.42$ was found for the square using a more exact describing function, S_1 .

It is readily seen that the buildup from zero amplitude to a maximum amplitude occurs along the respective curves, beginning at the linear theory intercept. To see this more clearly, refer to Fig. 3. The buildup is referred to the wind speed ratio U/U_c , the U_c being the "critical wind speed" found from the linear theory.

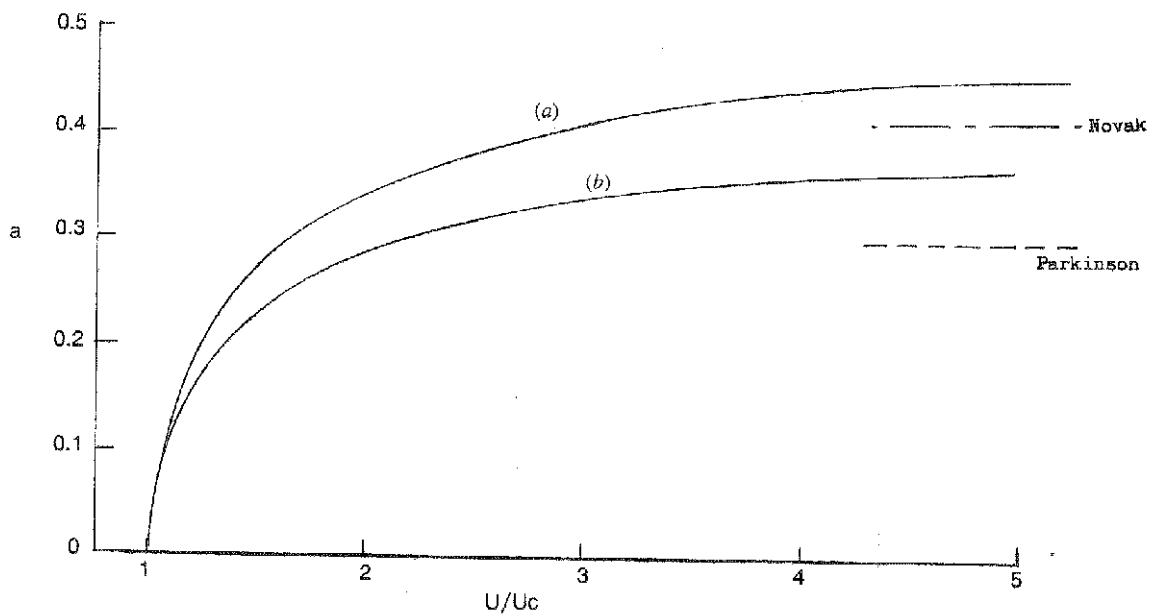


FIG. 3. Angle of Attack Buildup for Square Section, $\alpha_0 = 0$

If the system were equal in all other respects—except for $C_L \max$ —the U_c of the low Reynolds number system would be nearly twice the U_c of the high Reynolds number system. In Fig. 3, both curves start from a common point, but on a scale of wind speed the two curves would be separated along the abscissa.

It is seen that the buildup is rapid, once the critical wind speed is reached. However, while more than 50% of the “free-running” buildup is achieved at a wind speed only 50% above the critical wind speed, the remaining 50% of the buildup requires more than five times the critical wind speed.

For comparison, the approach to the “free-running asymptote” is shown relative to test data of Parkinson (1963) and Novak (1976). The asymptote for the “free-running” limit cycle at zero mechanical damping is found by putting the left-hand side of Eq. 10 equal to zero and solving the resulting transcendental equation

$$A_m J_1 \left(\frac{\pi a}{a_0} \right) [J_0(a) - J_2(a)] = C_D J_1(a) \dots \dots \dots (12)$$

The numerical value found for a is seen to be a function of both $C_L \max = A_m$ and the lift reversal angle ($= a_0$), as well as the drag coefficient, C_D .

To the extent that certain shapes may be “more” or “less” subject to large amplitudes of gallop, one could study Eq. 12 according to the various shape characteristics of lift and drag. Such a study would provide a basis for selection among the various alternative shapes (Richardson 1986).

CONCLUSION

The describing function method has been applied to single-degree-of-freedom systems with damping. The damping required to prevent gallop agrees with the linear theory when the amplitude approaches zero. The same critical wind speed is found. When the system damping approaches zero, or when the wind speed exceeds the critical wind speed by a factor of four to five,

the amplitude of gallop is the same as the "free-running" amplitude limited only by aerodynamic drag. A convenient approximate describing function is introduced, having only the following two parameters: (1) The maximum (negative) lift coefficient; and (2) the angle of attack for lift reversal. The effects of non-uniform aerodynamic force distribution remain to be considered, as do the effects of twisting. Since Reynolds number affects lift, critical wind speed may vary by as much as a factor of two on that account alone. Wind stream turbulence effects remain to be considered. However, lift and drag data having such effects included may be used within the framework of the present theory.

APPENDIX I. REFERENCES

- Jahnke, E., and Emde, F. (1945). *Tables of functions with formulas and curves*, 4th Ed., Dover, New York, N.Y., 150.
- Mukhopadhyay, V., and Dugundji, J. (1976). "Wind excited vibration of a square section cantilever beam in smooth flow." *J. Sound and Vibration*, 46(3), 329.
- IBID, Addendum, (1978), 56(2), 309.
- Novak, M. (1972). "Galopping oscillations of prismatic structures." *J. Engrg. Mech. Div.*, ASCE, 98, Feb., 27.
- Parkinson, G. V. (1963). "Aeroelastic galloping in one degree of freedom," *Paper 22*, First Symp. on Wind Effects on Buildings and Structs., Teddington, England, June 26-28, 582.
- Richardson, A. S., Martuccelli, J. R., and Price, W. S. (1963). Research study on galloping of electric power transmission lines," *Paper 7*, 1st Symp. on Wind Effects on Buildings and Structs., Teddington, England, Jun. 26-28, 612.
- Richardson, A. S. (1986). "Bluff body aerodynamics," *J. Struct. Engrg.*, ASCE, 112(7), 1723.
- Richardson, A. S. (1988). "Predicting galloping amplitudes: I," *J. Engrg. Mech.*, ASCE, 114(4), 716-723.
- Simiu, E., and Scanlan, R. H. (1986). "*Wind effects on structures*," 2nd Ed., John Wiley & Sons, New York, N.Y., 215.

APPENDIX II. NOTATION

The following symbols are used in this paper:

- A = Reference area for aerodynamic coefficients;
- a = maximum dynamic angle of attack;
- A_m = maximum static lift coefficient;
- a_0 = lift reversal angle of attack;
- C_D = drag coefficient;
- C_L = lift coefficient;
- $C_L \text{ max}$ = maximum lift coefficient;
- d = reference diameter;
- E = energy per cycle;
- f = frequency;
- g = structural damping;
- J_i = Bessel function of first kind, of order i ;
- m = mass per unit length;
- q = dynamic aerodynamic pressure;
- $q = 1/2 \rho U^2$
- S_l = describing function for lift;

t = time;
 U = wind speed;
 U_c = critical wind speed;
 Y = maximum gallop amplitude;
 α = angle of attack, instantaneous;
 α_0 = angle of attack, initial;
 δ = log decrement ($=\pi g$);
 μ = relative density [$=m/(1/2\rho d^2)$];
 ρ = air density; and
 Ω = radian frequency ($=\omega_v$).